

VISUALIZATION AND MEASUREMENT OF HELICOPTER ROTOR FLOW USING PROJECTED SMOKE FILAMENTS AND DIGITAL IMAGE PROCESSING

R. H. G. Müller*

Abstract

This paper presents an application of a new flow visualization method to complex flows over helicopter rotor blades. This method is based on the ideas of Dr. J. S. Steinhoff (UTSI) (Ref. 1). With the method, qualitative determination as well as quantitative measurements of the airflow are possible. The basic idea of the method is to produce thin, sharp-edged smoke trails by shooting very small burning metal pellets through the region of interest at high speed. These smoke traces can be placed as initially straight lines in any region of the helicopter rotor, even intersecting the rotor disc. After they are produced, the smoke traces follow the flow. The images of these traces in multi-exposure or multi-flash photographs then give a visualization of the flow field. The complicated nature of the helicopter rotor flow which can be visualized with the technique will be presented by several photographs showing, for example, the early stages of development of a tip vortex and turbulent flow patterns. In addition, the possibility of obtaining quantitative information about the flow field will be described. Digital image processing techniques are very helpful for this task. After digitization the smoke line images are accessible to the computer. Using different automatic or half-automatic procedures and the photographs taken stereometrically, the 3-dimensional flow field can be reconstructed.

Introduction

Flow visualization has, for many years, been an important tool in the study of complex fluid flows. Visualization pictures of the flow field allow many qualitative features to be determined relating, simultaneously, to the entire field. Also, in some visualization techniques, the possibility exists to obtain relatively accurate quantitative measurements of the flow field. The alternative to visualization is to measure flow quantities point-by-point using a probe or Laser velocimetry (Ref. 2,3). At a helicopter rotor flow field, these measurements are restricted to measurements of the mean values of flow velocities over many rotor revolutions. This may raise problems due to the relative large unsteady movements of the blades (for example the flapping angle).

In addition to the above, probe-based methods can have other disadvantages such as the creation of significant flow disturbances with hot-wire techniques and the requirements for seeding for laser velocimetry. It may never be possible to look at the de-

velopment of the flow from one point to another by means of the latter methods. This desirable Lagrangian view of the flow patterns, however, is provided by many flow visualization methods. In this paper, the application of a new flow visualization method will be described which has several advantages over currently used methods. First, a short description of this new method will be given. A more detailed description together with a comparison to existing visualization methods can be found in Ref. 4 and 5. In a very large scale experiment a similar although cruder visualization using small rockets has been performed (Ref. 6). Using digital image processing techniques, it is possible to reconstruct the flow field and calculate velocities and streamlines. Detailed results will be presented for a complex helicopter rotor flow field.

The method is based on the idea to produce, at one instant, an initially straight line of smoke within the flow at an arbitrary direction or location, normally perpendicular to the main flow. The smoke particles in this smoke trail are very small and follow the airflow very closely. Their motion can be used to determine the flow velocities normal to the smoke trail and, under certain circumstances, also along the trail. The smoke traces have sharp edges, are very thin (less than 0.5mm), can cover distances greater than one meter, and can be placed almost anywhere in the flow field. They are created by heating very small titanium pellets and projecting them through the flow. Due to the heating the pellets are burning and produce a trail of dense, white titanium dioxide smoke. This smoke fills the wake of the pellet, giving a diameter of the smoke trace that equals the dimensions of the wake, which is of the order of the size of the pellet itself. The disturbance of the flow induced by the particle and its wake is apparently very small and can be neglected, since when the trace is being observed, the pellet has gone beyond the observation region a distance several orders of magnitude greater than its diameter and all disturbances in the wake have decayed. Using a stroboscope or several triggered flashes, the light scattered by the smoke can be photographed. Flow velocities can be determined by measuring the displacement of the smoke traces between subsequent flashes.

Principle of the Method and Experimental Setup

As mentioned earlier, the method is based on the idea of shooting a burning pellet in an arbitrary direction into the air flow. This particle leaves a smoke trace with a sharp border which follows the flow. Titanium was chosen for the reason that it burns relatively slowly, does not vaporize at the temperatures involved, and produces an extremely dense white trace of titanium dioxide smoke. The shooting

*Independent Research Scientist; address: Dr.-Ing. Reinert H. G. Müller, Paul-Klee-Weg 8, D-4000 Düsseldorf 31, FRG.

mechanism consists of a thin glass pipette and works according to the principle of an exploding wire (Ref. 7 to 9) (see Figure 1). As can be seen in figure 1, a relatively large (1mm diameter) titanium pellet electrically connects two wires (standard wire wrap wire). The total resistance of the system is approximately 0.1 Ohms. Power is supplied by three 350 microfarad capacitors, which are charged to a voltage of 100V to 200V. (A "Slapshot IKS Pulser" from Plasma Research Corporation was used for the experiments.) Voltage rising time at the impedance of the shooter is about 10 microseconds. Due to the wire explosion the relatively large titanium pellet partially disintegrates into extremely small particles, which start to burn. The rest of the large pellet, which is of no further interest, and all the burning particles are accelerated by the explosion and leave the glass pipette at a speed of 200m/s and more, depending on the energy provided by the capacitors. At the distance of 0.33m an aluminum screen (figure 2) with a hole of 2.5mm diameter extracts one of these small particles, which then finally continues along its path through the region of interest in the flow. Due to this special screen arrangement, the probability is high that just one particle leaves the apparatus, or "Visualization Gun". Final particle speed is between 50m/s and 150m/s. If necessary for a high speed flow field, it is possible to extend the particle speed with the present apparatus up to about 250m/s. The particle, however, will slow down significantly due to the aerodynamic drag for longer shooting ranges.

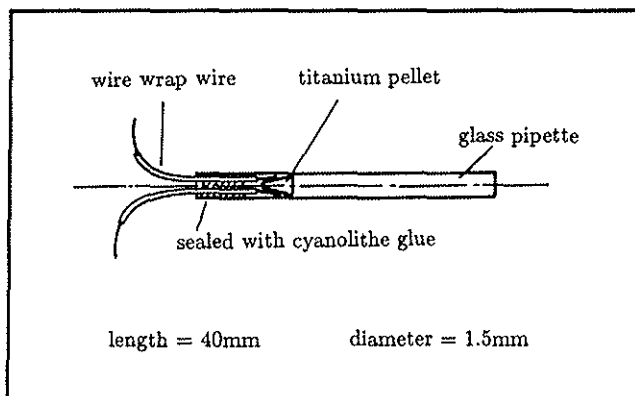


Figure 1. Glass pipette

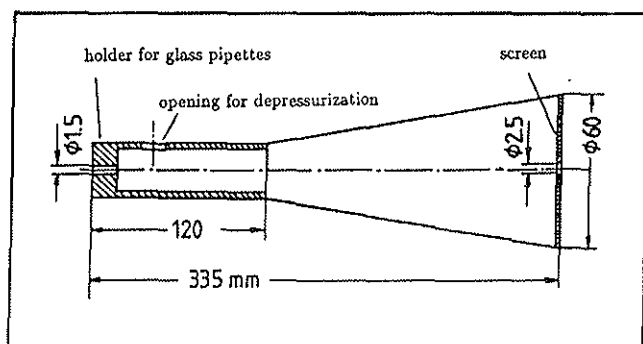


Figure 2. Visualization gun

Usable shooting distance with the gun was about 0.5m to 2.0m, depending on the particle speed, size, and temperature. After this distance, the particle becomes thermally unstable and disintegrates or explodes into a firework of even smaller particles.

Since the pellet is incandescent, it leaves a photographic image as it traverses the flow, separate from the illuminated smoke trail. Due to the drag forces on the pellet caused by the moving air, this image is not exactly a straight line. This effect can be large and influences the location of the smoke line. It is therefore not possible to place the line at an exactly determined position. The diameter of the pellet is less than 0.1mm and its wake and hence the smoke trace may extend to a width of less than 0.5mm. When the pellet has crossed the whole region of interest, the smoke trace is ready to be photographed. At this time, however, the trace is already influenced by the flow and by flow disturbances. This means that the older parts of the smoke trace have irregularities. This effect, rather than causing a problem, is helpful in determining the flow direction.

The smoke trace behaves like a time line and can be photographed in short time intervals. Leaving the camera shutter open, multi-flash photographs can be used to determine the local flow velocities by measuring the displacement of the smoke trace between two subsequent flashes.

For illumination of the smoke traces bright flashes are recommended. The particles of the titanium dioxide smoke are small ($< 1 \mu\text{m}$), and forward scattering illumination gives the best results (Ref. 10). At high flow speeds the time between two flashes should be very short. Maximum flow velocities measured in the experiments for this paper are about 20m/s, for which a flash timing of $\Delta t_{fl} = 0.6\text{ms}$ is used. These short time intervals are not possible with conventional repetitive high energy stroboscopes which must be recharged between flashes. Therefore, a set of up to four pre-charged triggered camera flashes is used (figure 3). Flash rising time is 0.1ms and decay time to half intensity is about 2ms. The duration of flashes partly determines the width of the visualized smoke lines. Due to the relatively long decay time the "leading edge" of the smoke traces, i.e., the edge in the direction of the flow velocity, is diffuse. The trailing edge, however, is very sharp due to the very fast rising time. Therefore, just the sharp trailing edge should be used for velocity measurements. Since there is one sharp edge, the relatively large width of the lines has no adverse effect on the images as long as the line images are not too close to each other.

For the helicopter rotor, two cameras (see figure 3) provided a three-dimensional view of the smoke lines. One of these (the side camera) was set to have a radial view towards the tip of the rotor blade, the other one (the top camera) was set to have a tangential view of the rotor, looking at the blade tip and the blade leading edge. The cameras were installed at special angles relative to the blade to provide as little surface light reflection as possible while keeping a good view of the smoke traces. The

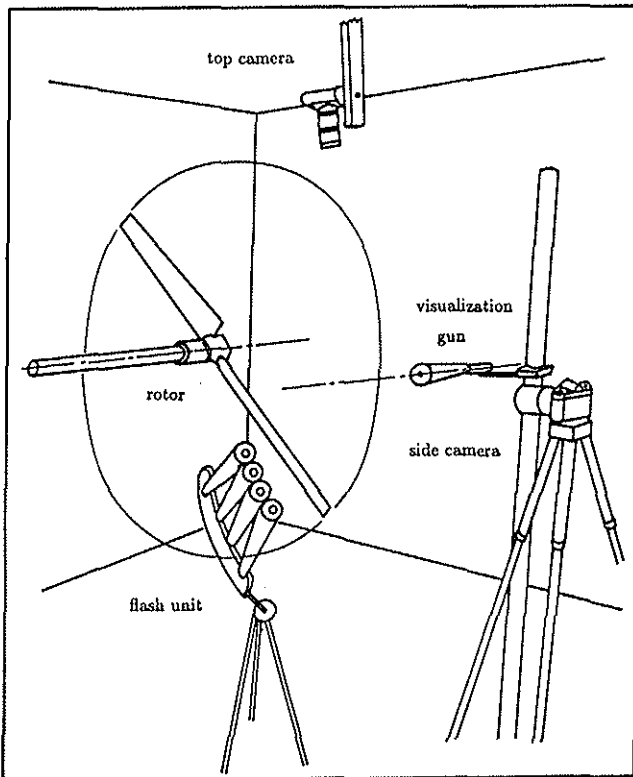


Figure 3. Experimental setup

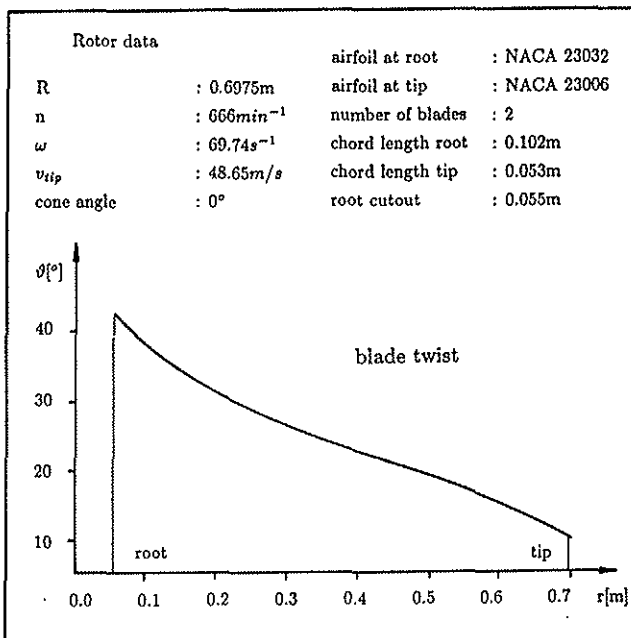


Figure 4. Rotor data

rotor used had two blades at fixed pitch, with 33° twist, and was 1.4m in diameter (see figure 4). The experiments were performed at a rotor speed of 666rpm, or a tip speed of 48.6m/s. This was actually a constraint of the available test rig. As can be seen in the smoke photographs, however, this should not be a limit for the method. The room used was not large enough to provide a hover flow field without ground or recirculation effects. The distance to all sur-

rounding walls was a little more than one rotor diameter. This, however, was not considered to be a problem because the main interest was the evaluation of the new visualization technique, not the detailed investigation of the new helicopter rotor in an undisturbed flow field.

Presentation and Discussion of the Flow Pictures

The helicopter rotor experiments were chosen to show the advantages of the new visualization technique, applying it to different complicated flow phenomena. Among these are tip vortices with high tangential velocities, turbulent regions in the flow field, and effects in the boundary layer of the blade, which are highly three-dimensional.

After a short qualitative discussion of the visualization photographs, a quantitative interpretation of the flow field will be given in the next chapter. Some of the problems in obtaining quantitative results are image distortions and low contrast, which can be overcome by means of the digital image processing techniques. Also, image processing will be used to combine two corresponding 3-D pictures.

As mentioned before, the cameras are set up to provide two different views of the flow field. Figures 5a,b show the principal flow fields for these two views for typical cases. The side view towards the tip shows the tangential velocities in the rotor disc and the flow distortions caused by the bound vortex in the blade. The top view towards the leading edge of the blade, on the other hand, provides a view of the radial flow at the blade and a good view of the developing tip vortex, if the smoke line is placed near the tip. The third direction, the axial flow, cannot be determined directly. However, it will be shown that it is nevertheless possible to obtain information about the axial flow by following recognizable distortions in the smoke trace caused by small scale flow distortions. The complex displacement of the smoke line in the side view, which is influenced by the bound circulation of the blade and the boundary layer, is explained in figure 6. To interpret the results, we imagine the flow as a relatively slow mean stream inward and downward, produced by the overall rotor wake. Then, the fast moving blade can be considered as a bound vortex moving through that flow.

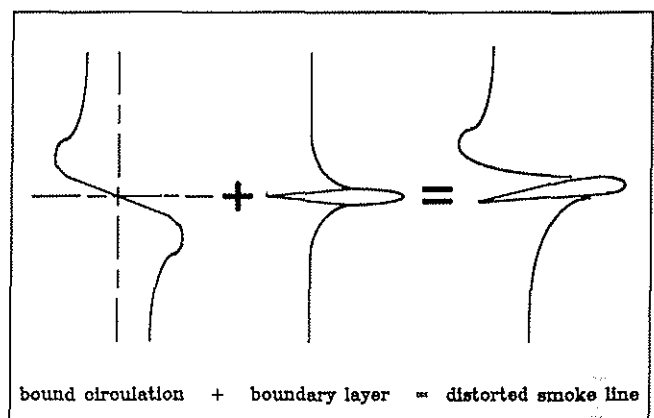


Figure 6. Superposition of influences

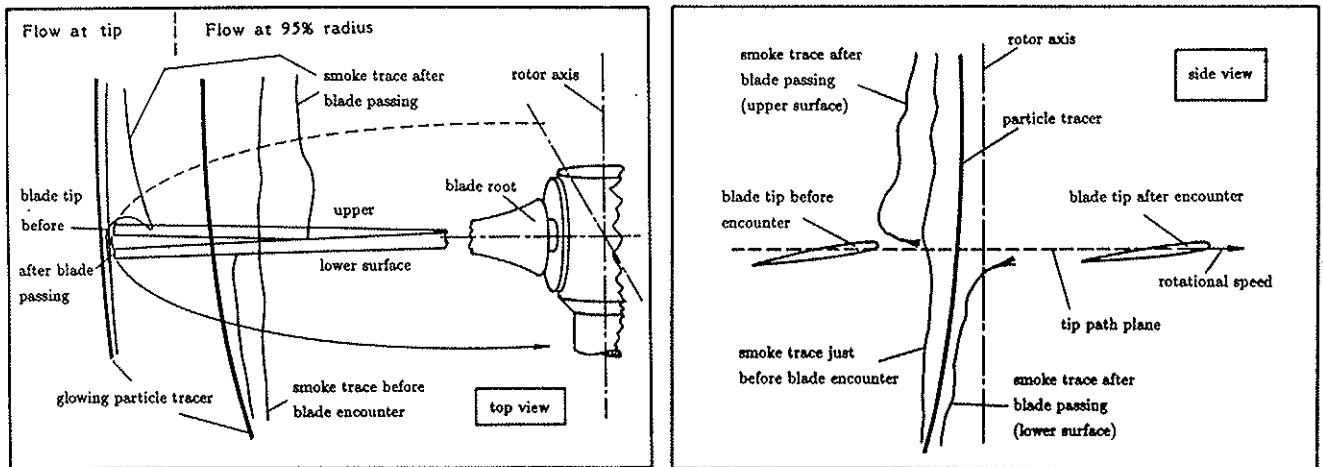


Figure 5a,b. Schematical flow field
(side view - radial; top view - tangential)

The effect of the blade will thus be a displacement of the smoke line, in the direction of the blade movement on the lower side and in the opposite direction on the upper side. In the boundary layer itself, of course, the blade will carry the smoke line in its direction. This can be observed in the photographs, at least in the outer part of the boundary layer, at absolute tangential velocities of up to $v_t = 10\text{m/s}$.

The first flow pictures in this presentation show the flow at a blade radius of 95% (figure 7). As shown in figure 5, in the top view the blade is turning towards the camera, in the side view from left to right. The time between the two flashes is $\Delta t_{fl} = 1.8\text{ms}$. The first flash is shot just before the blade passage and the second just after the blade passage. Additionally to the effect of the bound circulation and the boundary layer, several small distortions of the smoke line

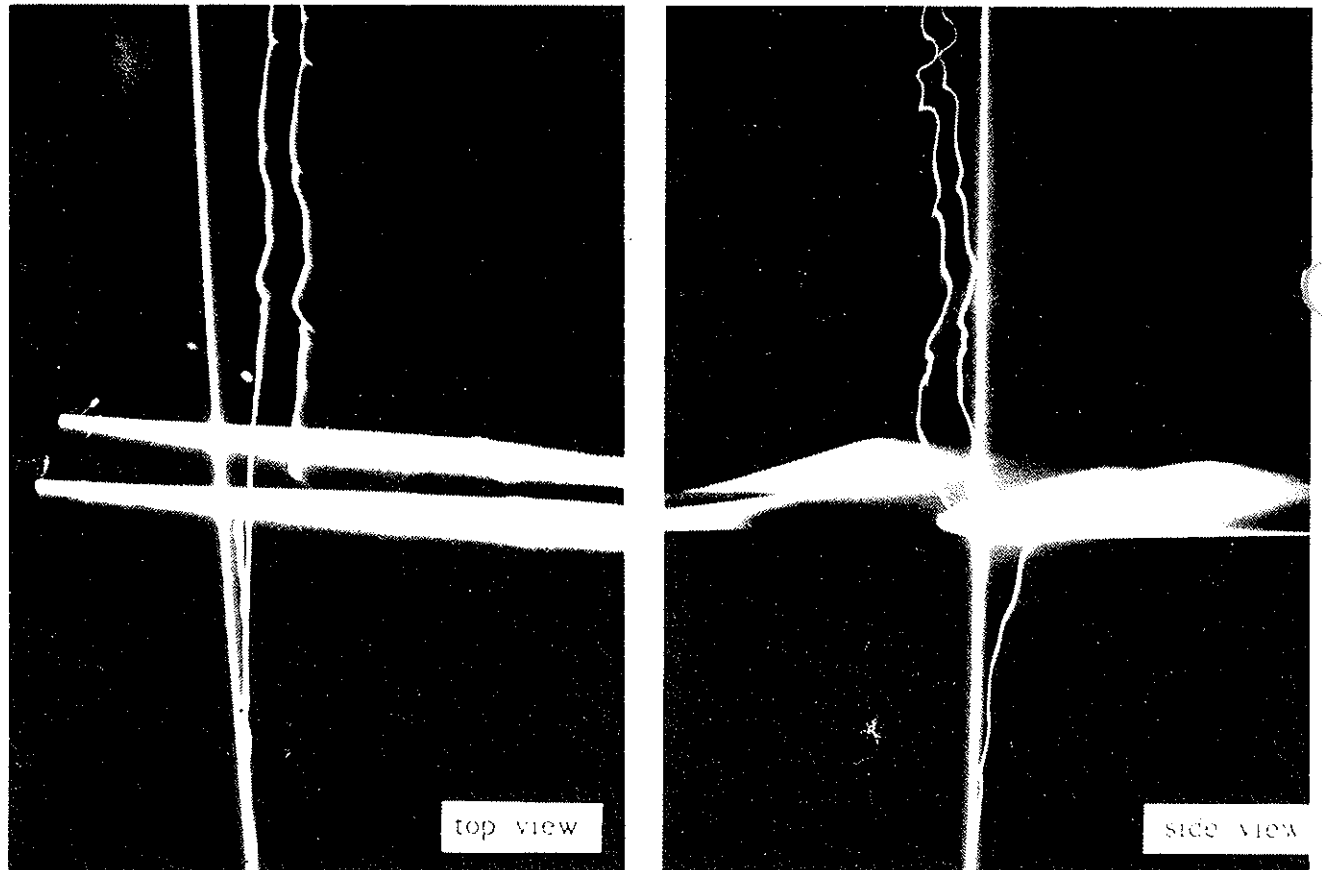


Figure 7a,b. Flow at 95% radius (2 flashes)

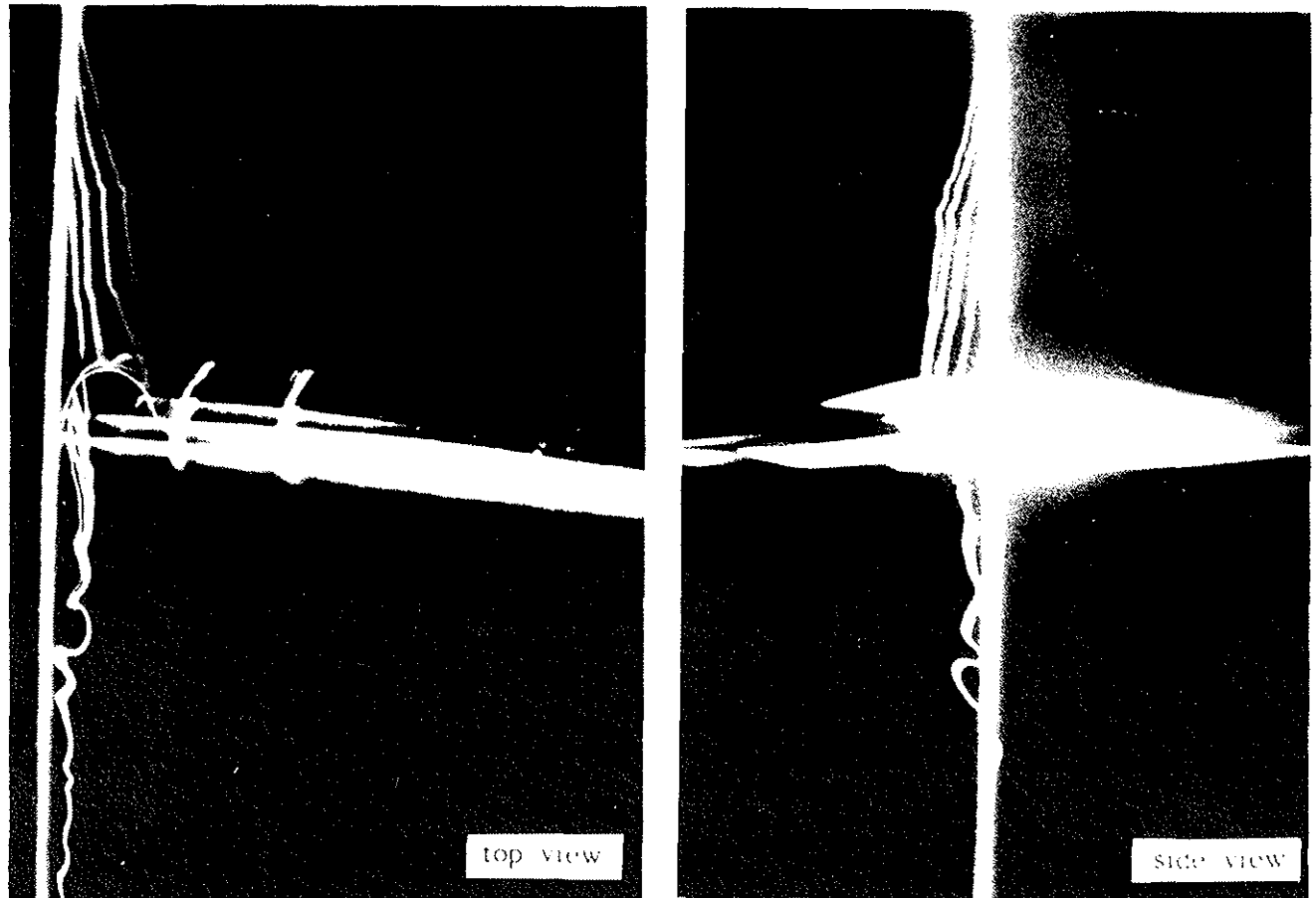


Figure 8a,b. Flow at blade tip (4 flashes)

images can be recognized, especially on the upper halves of the photographs. In figure 8, a four flash sequence is presented which shows the flow at the very tip of the blade. Due to the four flash sequence, four images of the blade can be seen. For figure 8, the initial smoke line was set very close to the tip at $\psi = 0^\circ$ at a time when the blade had an azimuth of about $\psi = -20^\circ$ (ψ is defined in fig. 3). Here, the influence of the developing tip vortex is very strong and the smoke line shows the location of the maximum tangential velocity within the developing tip vortex. There is very little distortion of the trace up to the encounter with the blade. At the first flash (at a blade azimuth of $\psi = -2.40^\circ$), the leading edge is very near to the still almost straight line. The distance between the initial line, represented by the incandescent pellet image, and the smoke line at the first flash shows an inward velocity, which represents the wake contraction. The next flashes, at blade azimuths of $\psi = 0^\circ$, $\psi = 2.40^\circ$, and $\psi = 4.80^\circ$, respectively, represent the flow field at about 25% chord and 75% chord of the blade, and a quarter chord after the trailing edge of the blade. Due to the fact that the vortex core develops somewhere inboard of the tip, there is no smoke inside of the core. Instead, the smoke stays exactly at that radius of the vortex, where it has encountered the vortex. This was just inside the radius of maximum tangential velocity, which can be determined as a mean value between each pair of smoke line visualizations. A quantitative interpretation of the tangential velocities will be presented later. In the side view

(Figure 8b), there is almost no influence at the lower side of the rotor disc, but there is a relatively large induced velocity of about 4 m/s at the upper side of the blade against the direction of the moving blade. This velocity extends to a large region more than one chord length over the blade.

Due to reflections from the blade, it is not possible with this four-flash-sequence to visualize the flow in the side view very close to the blade, especially in the boundary layer. This region may be, however, of great interest. Therefore two-flash-sequence images like figure 7 should be used for that purpose.

Digital image analysis and quantitative results

Using the smoke pictures to obtain qualitative statements and a better understanding of complex flow patterns only may already justify the effort of dealing with the described new method. A quantitative determination of the flow velocities or other flow properties, however, would be very desirable, especially for comparisons with other flow measurements or flow calculations.

As the method works according to the Lagrangian principle, two different approaches to get results are applicable: The first method is the determination of the flow velocities in one single photograph, i.e. at one single event and at one single location. This can be useful to determine, for instance, the development of the tip vortex with high accuracy. The second

method is the determination of a larger averaged flow field, using many photographs of the specific flow region, for example the tip region of the helicopter rotor. Examples for both methods will be described later on.

First, however, it is necessary to explain the process of determination of the flow velocities in the smoke pictures. As described in the last chapter, the displacement of any two adjacent smoke line images in one picture directly gives the mean flow velocity and flow direction between the two line images. The fact that all determined velocities are mean values between two adjacent line images may cause inaccuracies. Shorter time steps between two flashes than the used $\Delta t_{fl} = 0.6\text{ms}$ would help to get around this problem. Faster decay time of the light emission would be necessary yet. A good survey of different error considerations for methods using "time lines" like the smoke line images can be found in Lusseyran (Ref. 11).

Using the two corresponding images (top view and side view), however, only yields two components of the velocity. As the titanium particle and therefore the smoke line is shot in z-direction, displacements in x- and y-direction can be measured and give the velocity components v_x and v_y . To enable the determination of the velocity component in z-direction, additional information is necessary. One way to obtain these information could be an additional smoke line placed in a different direction. This, however, is not possible at the current state of development of the method. The method is not yet reliable enough to enable the production of two good and straight smoke lines at the same time at predetermined direction. However, another feature of the smoke lines can give the desired information: Due to flow disturbances, turbulences or little vortices, the smoke lines develop little edges, vertices, or loops. These normally very small distortions or deficiencies grow larger during the observation time between the two or four flashes. However, they do not change their shape very much within the time step between each two flashes and can be recognized at each subsequent flash. This means a little loop may grow larger, but it will stay a loop even after the observed time period of usually 1.8ms. An edge or vertex may change its shape and get sharper or smoother but can be recognized in each line image at each flash.

These little deficiencies, called "reference points", can be used to determine the flow velocities in the direction of the smoke line.

The number of smoke pictures to analyse is very large. Therefore, a determination of the displacements of the lines by hand is almost impossible. Digital image processing methods can be used to make this task easier. The pictures are digitized in a spatial resolution of 512×512 picture elements (pixel) and 256 grey levels. The part of the image which is digitized has a size of $12\text{cm} \times 12\text{cm}$. This gives a resolution of 4.27 pixel/mm. Using a flash time distance of $\Delta t_{fl} = 0.6\text{ms}$, this results in a velocity resolution of 0.4m/s . This is enough for the expected

velocities of 10 to 20m/s and can be extended easily by using higher camera resolution up to 1024×1024 pixel or by grabbing smaller parts of the picture at higher resolution. To minimize the noise of the camera and the analog-digital-converter, the mean value of 64 image acquisitions has been calculated for each final picture. Only 4-flash-sequence images have been chosen for the later interpretation to give as much information as possible. Even these 4-flash-sequence images result, for a single photograph, only in the quite low resolution of 4 points or 3 mean values of the velocity in normal direction to the smoke line at each vectorized line point. Using a large number of smoke line photographs at different flash sequences and with small variations in the rotor azimuth, however, enough velocity values can be collected to reconstruct the whole flow field. For these kinds of visualizations the time steps of 0.6ms between two flashes are relatively large (the blade moves almost half a chord in azimuth within that time step). With the availability of shorter flash decay times, it will be possible to use shorter time steps of 0.2ms or less.

24 pairs of pictures (top and side view) of the outer 15% of the blade have been chosen for further interpretation. After scale correction and rotation to the camera-orientated, tip-path-plane-fixed $x'y'z'$ -coordinate system in figure 9, top view and side view can be combined on the computer screen to a picture like figure 10. The side view, which shows the $x'z'$ -plane, is located on the left hand side, the top view, which shows the $y'z'$ -plane, is located on the right hand side. The pictures are shifted until the origin is located at the same screen-y-coordinate. The origin is defined as the image of the trailing edge of the blade tip at the last flash.

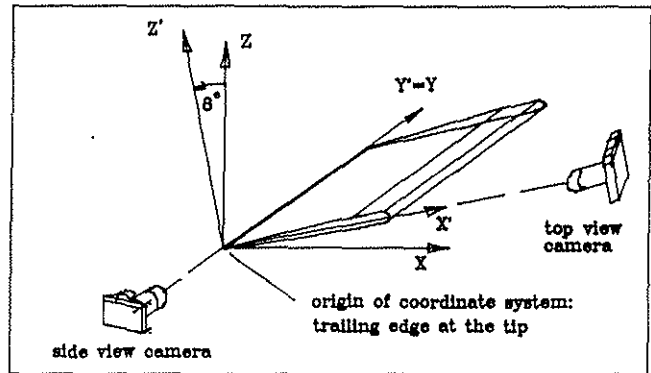


Figure 9. Coordinate systems

The next step would be the vectorization of the smoke line images and the reference points on the lines. In future works, this will be done using completely automatic working image processing techniques like edge detection, line extraction, line erosion, and vectorization. These techniques are available as subroutines in most of the image processing systems on the market. Due to difficulties like line crossings or intersections or line contacts, disturbing blade

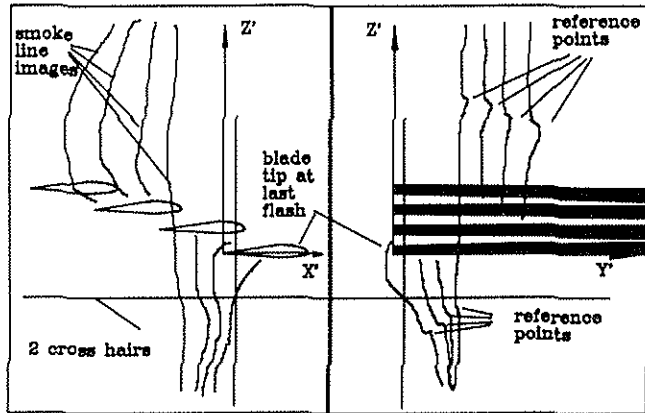


Figure 10. Combined picture on the computer screen

parts or disturbing smoke lines, produced by other, accidentally placed titanium particles, this automatic vectorization was not yet operational for the work described here. Instead, a half automatic procedure was chosen: after simple image enhancement procedures (Laplace-filter), the vectorization was performed on screen by hand using two cross-hairs, one in each of the two views. After determining the origins of the $x'y'z'$ -coordinate systems in each half picture (window) and after input of the scale factor of 4.27 pixel/mm the vectorization was done by just clicking on corresponding points in each view of the smoke line images with the cross-hair pointer. For easier operation the two cross-hairs were attached to each other in the screen- y -coordinate, which is the z' -coordinate in the camera-orientated system. A move of one cross-hair in that direction would pull the other in the same direction. Reference points are marked specially, the number of regular points between two reference points may be as large as necessary to give a good reproduction of the line image. Depending on the complexity of the lines the vectorization was done with 50 to 100 vectors per line and 5 to 10 reference points per line.

After complete vectorization of a set of four lines the number and position of vectors for each line was adjusted automatically by linear interpolation of extra points and shifting them between each two reference points. Extrapolation was used to adjust the length before the first reference point and after the last one. Both these processes were done in respect to the longest and most complex line of each set. This guarantees the integrity of the complicated shape of all lines of a set.

After a rotation and shift to the blade-fixed x,y,z -coordinate system, these vectorized lines were used to calculate the mean velocities between each two corresponding points of each two adjacent vectorized lines. This has been done for the tip vortex velocity in figure 11. An aging of the vortex core is shown in the figure which occurs before the vortex has completely developed. Up to 65% of the blade chord, the radius of the largest tangential velocity v_{tan} is located at $r_{core} = 9\text{mm}$, which is about 17% of the blade chord. Later, in the vicinity of the trailing edge, this radius grows to about $r_{core} = 11\text{mm}$ (23% of the blade chord). In the starting phase the tan-

gential velocity maximum shows a sharp peak, later at the trailing edge, the peak becomes wider and weaker. For comparison, an enhanced and blown up image of the vortex core is shown in figure 12.

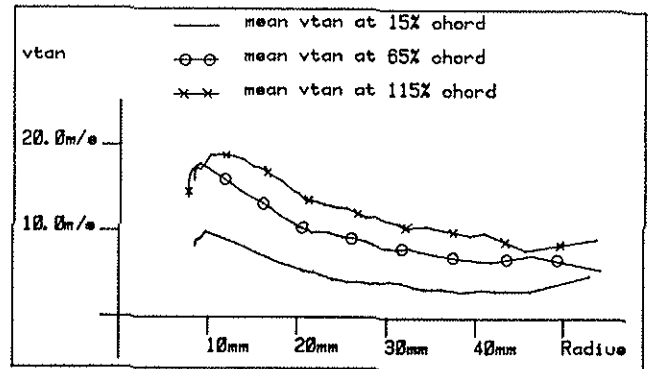


Figure 11. Tangential velocities in the tip vortex

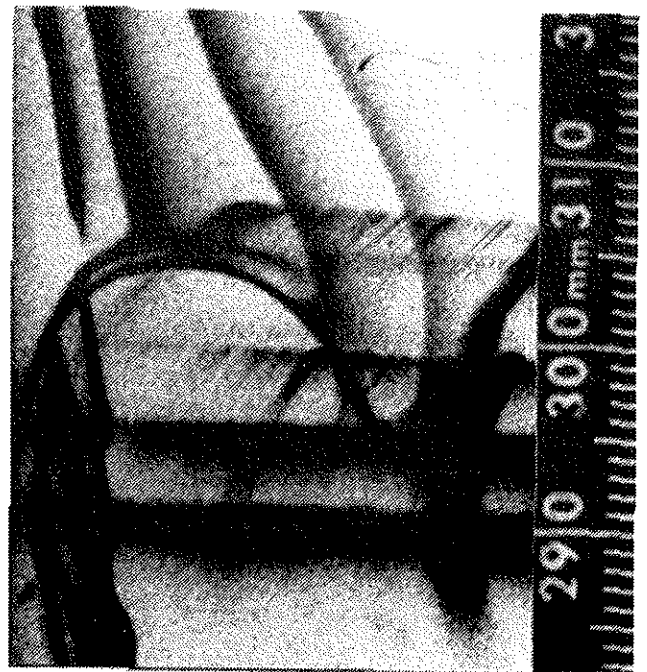


Figure 12. Enhanced image of the vortex core

No other method would enable these measurements at the blade tip, especially as the measured tip path plane shows vertical variations (out of the regular tip path plane) of 10mm, which is of the order of magnitude of the vortex core itself. An LDA-measurement, which necessarily would be a procedure of taking mean values of many rotor revolutions, could hardly give a similar reproduction of the tip vortex. The Lagrangian view of the flow field, taken at a single blade encounter, seems to be the only possibility to show the development of the tip vortex at a rotating rotor blade.

Another way to present the flow field is the plot of streamlines (see figure 13) or velocity fields. To enable comparisons with other measurements or with flow calculations, the velocities at every point of the measured volume should be available. This can be achieved by a 3-dimensional inter- and extrapolation process.

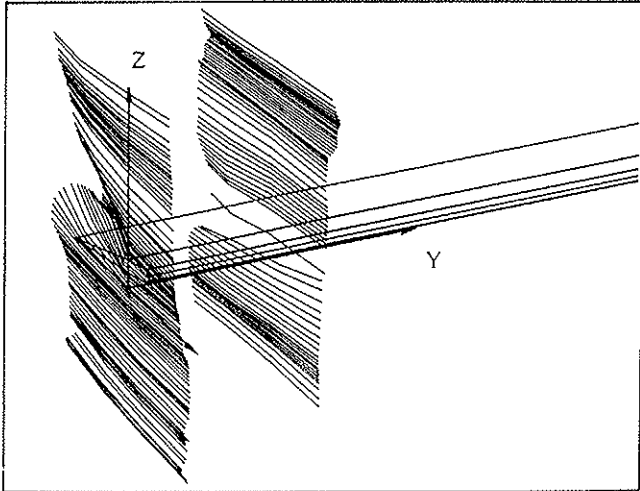


Figure 13. Streamlines at different radial station

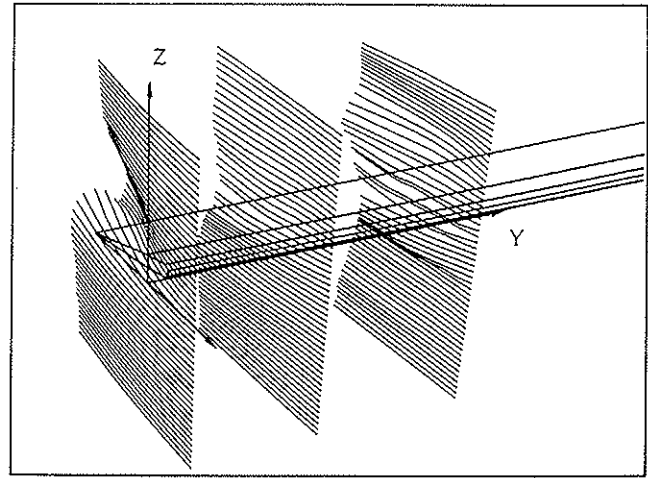


Figure 15. Interpolated streamlines

When performing such a process, it is important to remember that each pair of pictures or set of smoke line images presents a single flow field at special conditions (unsteady blade twist, flapping angle, disturbances by vortices and turbulence). The combination of the 24 vectorized sets of smoke line images necessarily gives a smearing of the tip vortex and the other flow field even if the movement of the blade is considered, i.e. if the origin of the coordinate system for each picture is fixed to the unsteady blade position.

The 3-dimensional interpolation scheme is explained in figure 14: A cylindrical volume, orientated as close as possible in the direction of the streamlines in its vicinity, is divided into eight octants. Only points located in this cylinder are considered to form the interpolated value for the center of the cylinder. Each of the octants has the same weighting, independent of the number of measured points within the octants. Additionally to the weighting scheme of the eight octants, there is a distance-depending weighting of the velocities at each measured point. Results of this interpolation are plotted in the next figures as streamline- or velocity-plots.

In figure 15 the interpolated streamlines are shown from the same point of view as in figure 13. As expected and explained earlier, the tip vortex roll-up looks a little smoother in the interpolation compared to the direct measurement in figure 13. However, the

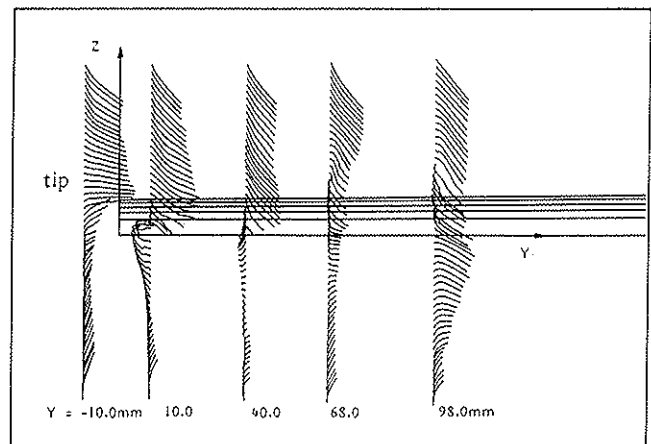


Figure 16. Interpolated streamlines (y,z-plane)

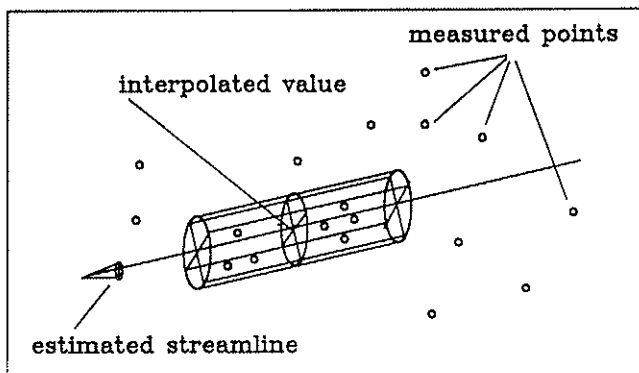


Figure 14. 3-dimensional interpolation scheme

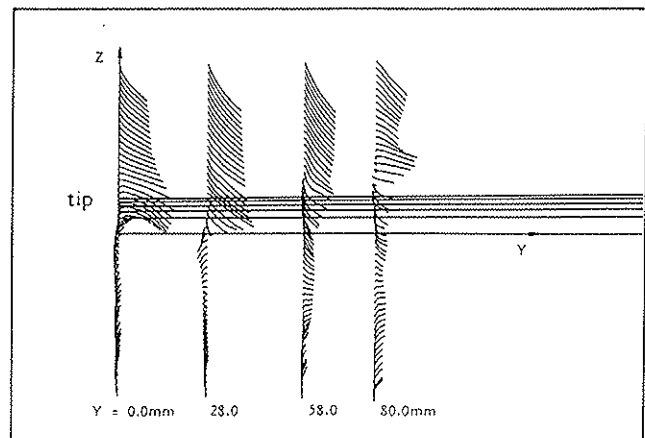


Figure 17. Interpolated streamlines (y,z-plane)

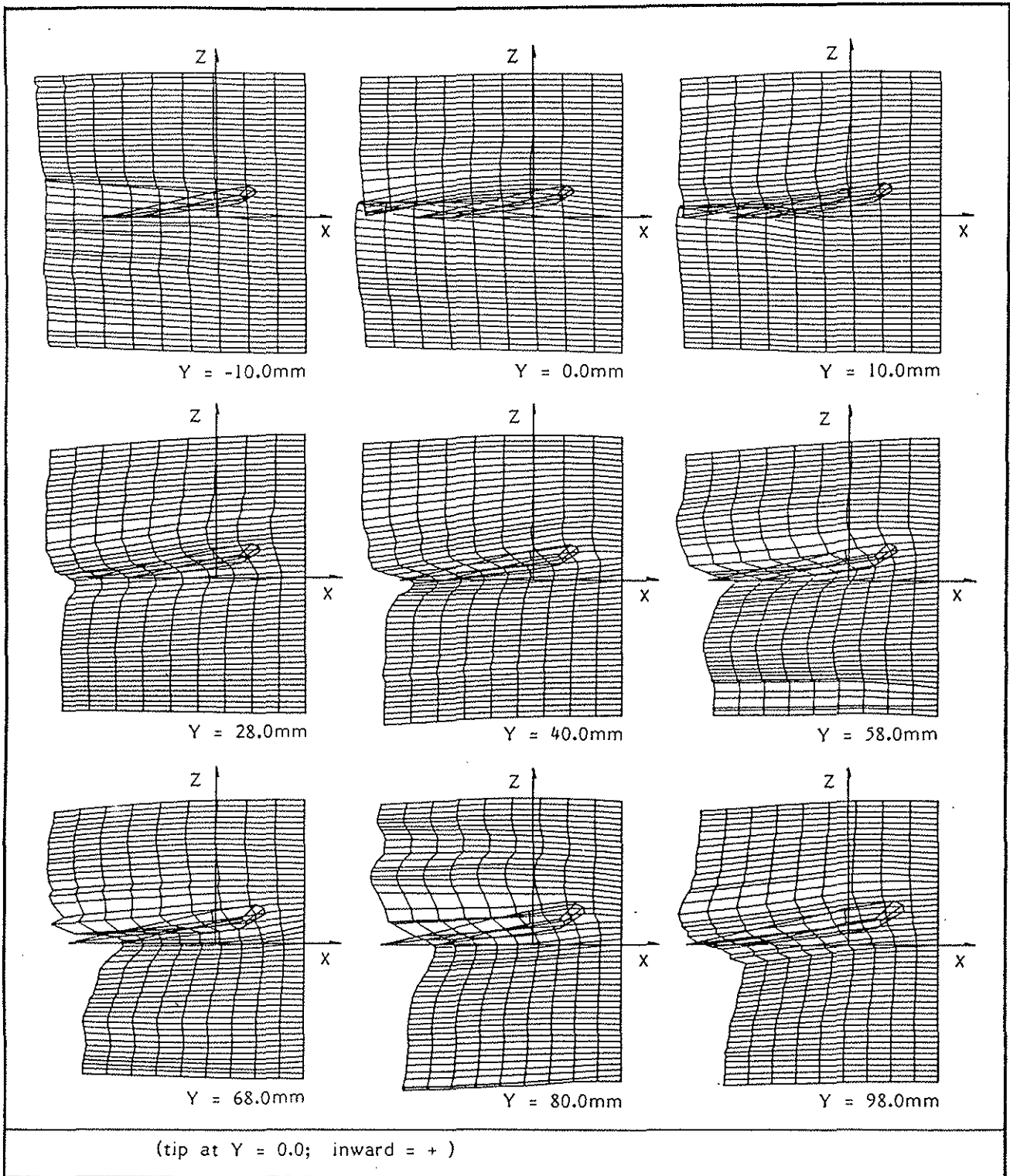


Figure 18. Interpolated streamlines (x,z-plane)

agreement is still good and proves the reliability of the interpolation method even at the high velocity gradients at the tip vortex. Figures 16 and 17 show streamlines in the y,z-plane, facing the leading edge of the blade, at different radial blade stations. Figures 18 and 19 show streamlines and velocities in the x,z-plane, facing the tip of the blade. Velocity losses behind the trailing edge can be observed in figure 18, the velocities induced by the bound

circulation of the blade in figure 19. Using these velocities, the bound circulation of the blade can be calculated (see figure 20). The slope of the bound circulation is not very smooth due to the differences in the flow conditions of the 24 pairs of pictures used for this interpolation. These interpolated values may serve to validate theoretical flow models like the free wake analysis method described in Refs. 12 and 13.

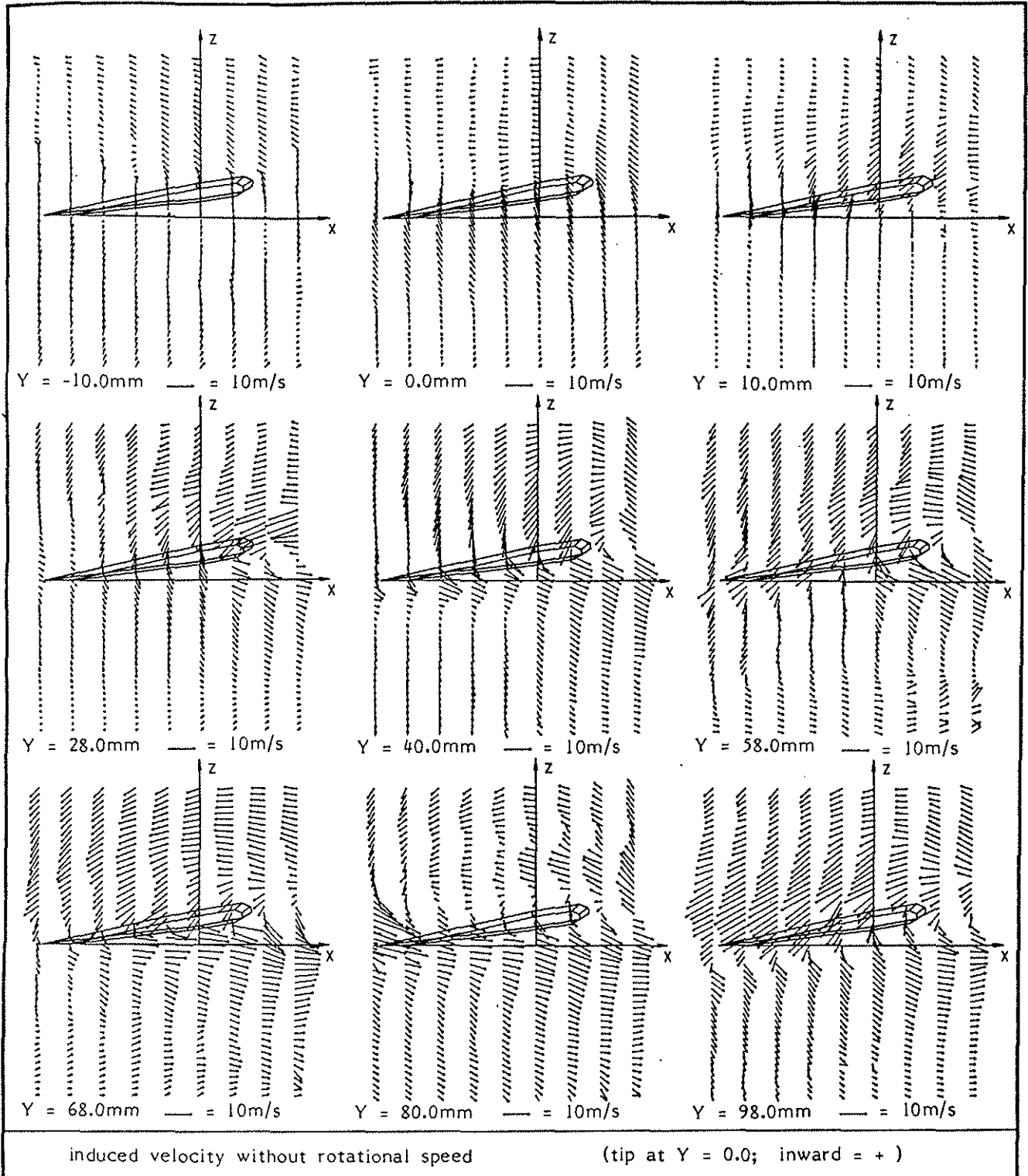


Figure 19. Interpolated velocities (x,z-plane)

Turbulence

The reference points used for the determination of the velocities in direction of the line itself can be taken for effects of little vortices or turbulence. Such instabilities, for instance little loops in the smoke line images which can be observed over relative long time periods, could help to interpret the complicated behaviour of turbulent flow patterns. By

means of the usual methods, these patterns can be determined only statistically. Using the Lagrangian view combined with the sharp smoke line images of the new method, completely new interpretation possibilities will arise. An example is given in figure 21, presenting a flow field at a time interval of 5.4ms ($\Delta t_{fl} = 1.8ms$, four flashes, two smoke lines result in eight line images).

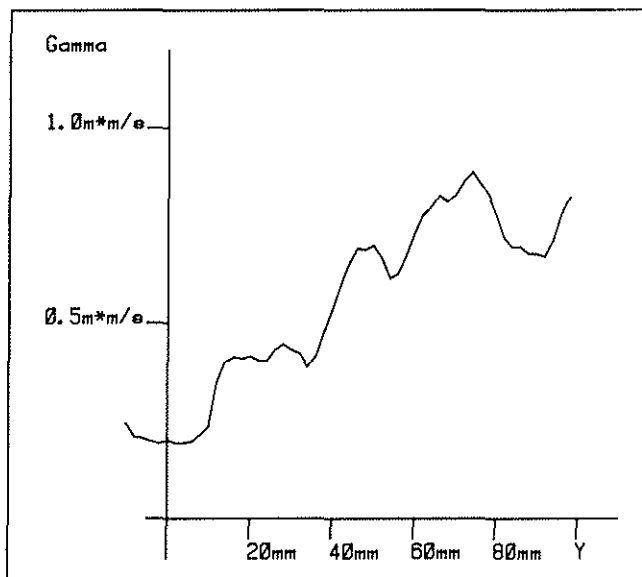


Figure 20. Bound circulation of the blade tip

Conclusion

The application of a new flow visualization method is presented, which enables the qualitative and quantitative interpretation of complex time dependent flow fields. As an example, the application to a very complicated helicopter rotor flow is shown. The visualization pictures show, for example, the just developing tip vortex with tangential velocities of up to $v_t = 20\text{m/s}$. Using digital image processing techniques, a quantitative determination of streamlines and flow velocities in the flow field around the helicopter rotor blade is possible. As examples, the velocity distribution in the tip vortex and the bound circulation distribution on the blade are presented.

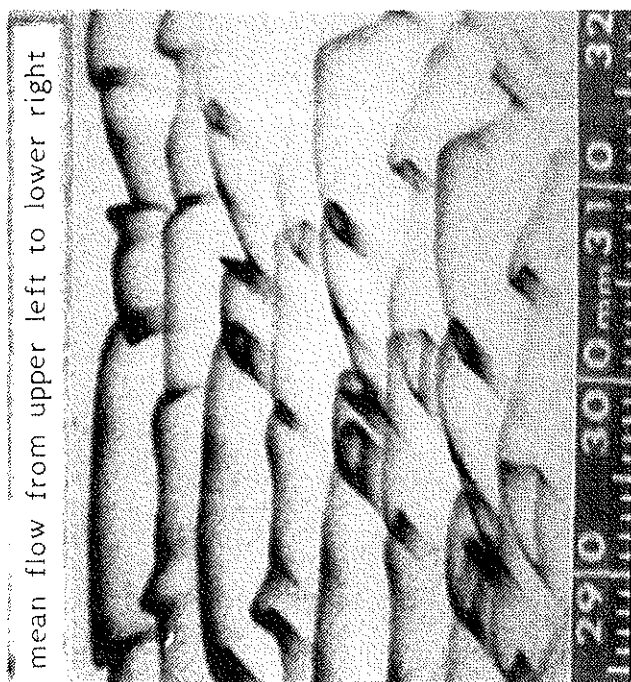


Figure 21. Turbulent or vortical flow patterns

Acknowledgements

The author would like to thank Dr. J. Steinhoff for the initiation of this work. This project was supported by the Deutsche Forschungsgemeinschaft (DFG) and The University of Tennessee Space Institute (UTSI) and the Johanna-und-Fritz-Buch-Gedächtnis-Stiftung. Many thanks are due to Dr. Silke Hasenclever and Dipl.-Phys. Thomas Fränz for discussions of the work and corrections of the text.

References

1. Steinhoff, J. S., "A Simple Efficient Method for Flow Measurement and Visualization," Flow Visualization III, Hemisphere Publishing Corporation (1985) Springer-Verlag, Edited by W. J. Yang, pp. 19-24.
2. Lorber, P.F., Stauter, R.C., Landgrebe, A.J., "A Comprehensive Hover Test of the Airloads and Airflow of an Extensively Instrumented Model Helicopter Rotor," Proceedings of the 45th AHS Annual Forum, May 1989.
3. Thomson, T.L., Kwon, O.J., Kemnitz, J.L., Komerath, N.M., Gray, R.B., "Tip Vortex Core Measurements on a Hovering Model Rotor," AIAA 25th Aerospace Sciences Meeting, Jan.12-15, 1987, Reno, Nevada.
4. Müller, R.H.G. and Steinhoff, J. S., "Application of a New Visualization Method to Helicopter Rotor Flow," presented at the 8th AIAA Applied Aerodynamics Conference, Portland, Oregon, August 20-22, 1990.
5. Müller, R.H.G., "Eine neuartige Methode zur Visualisierung von Strömungen sowie Auswertung der Strömungsbilder mittels digitaler Bildverarbeitung," Abschlußbericht DFG (Deutsche Forschungsgemeinschaft) Mu 802/1-1, 1990.
6. Dewey, John M. and McMillin, D. J., "Visualization of Shock and Blast Wave Flows," Flow Visualization I, Hemisphere Publishing Corporation (1978) and McGraw-Hill, Edited by Tsnyoshi Asanuma, pp. 279-284.
7. Chace, William G., "Liquid Behavior of Exploding Wires," The Physics of Fluids, Vol. 2, No. 2, March-April 1959, pp. 230-235.
8. Scherrer, Victor E., "An Exploding Wire Hypervelocity Projector," Exploding Wires, Vol. 2, Plenum Press New York, 1962, pp. 235-244.
9. Bohn, J. L., Nadig, F. H., Simmons, W. F., "Acceleration of Small Particles by Means of Exploding Wires," Exploding Wires, Vol. 3, Plenum Press New York, 1964, pp. 330-351.
10. Van de Hulst, H. C., "Light Scattering by Small Particles," John Wiley and Son, New York, 1964.
11. Lusseyran, D. and Rockwell, D., "Estimation of Velocity Eigenfunction and Vorticity Distributions from the Time Line Visualization Technique," Experiments in Fluids 6, pp 228-236 (1988).
12. Müller, R.H.G., "Der Einfluß von Winglets an Rotorblattspitzen auf die Strömungsverhältnisse am Hubschrauberrotor," Diss. RWTH Aachen, Fortschrittberichte VDI Reihe 12 Nr. 108, VDI-Verlag 1988.
13. Müller, R.H.G. and Staufienbiel, R., "The Influence of Winglets on Rotor Aerodynamics," Vertica Vol 11, No 4, pp 601-618, 1987.